Food Chemistry: X 20 (2023) 100931

Contents lists available at ScienceDirect

Food Chemistry: X

journal homepage: www.sciencedirect.com/journal/food-chemistry-x

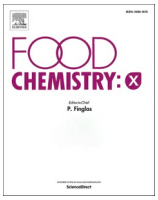

# The influence of α and α′ subunits on SPI Pickering emulsions based on natural hybrid breeding varieties

Chunmei Gu [a,b], Pengchao Dong [a,b], Feihong Jiang [a,b], Hongling Fu [a,b], Bo Lyu [a,b], Haoming Li [a], Youbao Li [a,b], Hansong Yu [a,b,*], Weichang Dai [a,b,*]

[a] College of Food Science and Engineering, Jilin Agricultural University, Changchun 130118, China
[b] Division of Soybean Processing, Soybean Research & Development Center, Chinese Agricultural Research System, Changchun 130118, China

ARTICLE INFO

*Keywords:*
Pickering emulsion
Soy protein isolate
Protein nanoparticle
Subunit deficiency

ABSTRACT

In this study, food-grade protein nanoparticles (Wild-NPs, α-lack-NPs, α′-lack-NPs, and (α + α′)-lack-NPs) were organized as emulsion stabilizers via thermal induction. The effects of α and α′ subunits in soybean protein isolate (SPI) on Wild nanoparticle Pickering emulsion (Wild-NPPEs), α-lack nanoparticle Pickering emulsion (α-lack-NPPEs), α′-lack nanoparticle Pickering emulsion (α′-lack-NPPEs) and (α + α′)-lack nanoparticle Pickering emulsion ((α + α′)-lack-NPPEs) were investigated. The Pickering emulsion stabilization mechanism indicated that the α′-lack-NPs particle size, surface hydrophobicity, and contact angle were mostly comparatively large. Therefore, the absence of the α′ subunit made the desorption of protein nanoparticles at the oil and water interface require higher energy. Through the hydrophobic interaction between molecules, the structure and properties of the emulsion were improved, showing good stability. The existence of α′-lack-NPPEs leads to the formation of a gel-like network in the emulsion, which increases the viscosity of the emulsion and makes the network structure of the emulsion more uniform and denser.

## 1. Introduction

Pickering emulsions contain solid particles that stabilize the emulsion, generally at the micron or nanoscale, called Pickering particles. The Pickering emulsion stability mechanism is different from that of traditional emulsions. The former stabilizes the oil–water interface through solid particles attached to it, increasing the spatial resistance and increasing the rheology of the nondisperse phases (Xiao, Wang, Perez Gonzalez, & Huang, 2016). The latter consists of amphiphilic surfactant molecules adhering to the interface to reduce interfacial tension and stabilize the emulsion system (Sun et al., 2022). In recent years, traditional emulsifier-stabilized emulsions have suffered from the disadvantages of inconvenient storage and high emulsifier usage, and Pickering emulsions that are stabilized by nanoparticles have been used by scientists in a wide range of different fields. However, more research has focused on the synthesis of inorganic polymer particles based on physics or chemistry, but these particles are non-biodegradability and non-compatibility for organisms (Li, Li, Huang, Luo, & Mei, 2021). The main solid particles that are not food-based are titanium dioxide (Amar Feldbaum et al., 2021), asphalt (Wang, Babadagli, & Maeda, 2021), silica (Slavova, Pollak, & Petermann, 2019), volcanic mineral clay (Aimable, Lecomte-Nana, & Pagnoux, 2022), and graphene (Ma et al., 2021). Therefore, because of environmental factors, the development of environmental protection, harmless, biodegradable food grade particles as Pickering emulsion stabilizers, has aroused great interest.

Proteins, as amphiphilic compounds with good surface activity, can be used as solid particles and are widely explored to enhance the traditional oil-in-water emulsions, formation of good interface adsorption, emulsifying properties, and stability. Given health, ethical, and environmental protection issues, the preparation of Pickering emulsion solid particles from plant proteins has become a significant hotspot in research. Pea protein isolate microgels were heated and homogenized with sucrose and sunflower oil to stabilize the edible mayonnaise-like Pickering emulsion (Li et al., 2022). The quinoa protein isolated Pickering high internal phase emulsion gel as an antifreeze for frozen foods is important for improving food quality (Cen, Yu, Gao, Feng, & Tang, 2021). To improve the bioaccessibility of astaxanthin, we prepared high internal phase Pickering emulsions (HIPPEs) based on Seabass protein (SBP) microgel granules and used astaxanthin-containing HIPPEs for rapid prototyping technology (3D printing) (Zhang, Xu, Zhao, & Zhou,

* Corresponding authors.
*E-mail addresses:* yuhansong@163.com (H. Yu), daiweichang@jlau.edu.cn (W. Dai).

https://doi.org/10.1016/j.fochx.2023.100931
Received 28 June 2023; Received in revised form 29 September 2023; Accepted 5 October 2023
Available online 10 October 2023

2022). The freeze–thaw stabilities of heated SPI and whey protein (WP) (nano) granule stable Pickering emulsions and unheated separated soybean protein (or WP) and sodium caseinate (sodium cyanide) were compared. These results of food protein granule stable Pickering emulsion preparation and its application in food formulas are of great significance (Zhu, Zhang, Lin, & Tang, 2017). SPI has good emulsification, gel, and foam properties (Huang, Lee, Wang, & Qiu, 2023). Heat-induced denaturation can alter the functional properties of SPI, leading to both the exposure and formation of hydrophobic amino acids and protein aggregates within the protein and affecting its solubility and emulsification (Guo et al., 2021). Differences in the structural composition of SPI can directly affect its processing characteristics and nutritional quality. Therefore, further analysis of the influence of subunit levels on the functional properties of gel is necessary and is more conducive to the industry trend of specialization of processed varieties.

In addition, our group has determined in preceding research that the different gel properties (Fu et al., 2023) and foaming residences (Li et al., 2022) of soy protein are due to α or α′ subunit deficiency. Therefore, it is of theoretical importance to explore the emulsification properties of soy protein at the subunit level to improve the utilization of soy protein. In this research, we analyzed the emulsification properties of SPI at the subunit level by thermally inducing subunit-deficient soy protein to prepare protein nanoparticles and analyzed and compared their particle size, ζ-potential, surface hydrophobicity, and contact angle to investigate the properties of the prepared Pickering emulsions. In this paper, we investigated the properties of Pickering emulsions of different subunit deletion kinds of soy protein. The improvement and future application of soy protein product additives provide a theoretical basis.

## 2. Materials and methods

### 2.1. Materials

Wild-type, α-lacking, α′-lacking, and (α + α′)-lacking soybeans were provided by the Key Laboratory of Soybean Biology in the Chinese Ministry of Education (Harbin, China). Soybean oil was purchased from a local supermarket (Changchun, China). 1-Anilinonaphthalene-8-sulfonic acid (ANS) (St Louis, MO, USA) and coomassie Brilliant Blue and sodium dodecyl sulfate (SDS) (Jinhua University Chemical Reagent Co. Ltd. Guangzhou, China) were used. All other chemicals and reagents for the analysis were from the Beijing Chemical Industry Group Co., Ltd. (Beijing, China).

### 2.2. Preparation of soy protein isolate (SPI)

Following the methodology studied by Li et al. (2022), the four kinds of soybeans were peeled, crushed, and screened for 60 mesh, and then the powder was mixed with acetone to prepare the defatted soybean powder. After repeating this process four times, the powder was dried. According to the principle of alkali-soluble acid precipitation, the degreased soybean powder was mixed with deionized water (1:10). The acidity and alkalinity of the solution were adjusted with 2 mol/L NaOH solution to pH = 8.5, and after 2 h of full agitation, 2 mol/L HCl solution was added, and the acid-base pH of the solution was adjusted to 4.5. After 2 h of full agitation, the pH of the mixture was adjusted to 4.5. The mixture was centrifuged for 30 min (14,000 g at 4 °C), and the precipitate was taken and redissolved in water several times. A 2 mol/L sodium hydroxide solution was added to adjust the acidity and alkalinity of the solution to pH = 7.0. After the mixed solution was stirred for 2 h, the supernatant was obtained by centrifugation for 30 min (14,000*g* at 4 °C). Dialysis was performed at 4 °C for 48 d and freeze-dried. Four proteins were labeled as Wild, α-lack, α′ -lack, and (α + α′) -lack for later data processing.

### 2.3. SDS–PAGE

The protein compositions of soybeans were analyzed by SDS–PAGE with some minor modifications to Laemmli (1970) method, and a 12% PAGE separation gel and 4% concentrated gel were prepared. At room temperature, each sample was spiked with 0.02% β-mercaptoethanol after heating (100 °C, 5 min) and centrifuge (10,000*g*, 5 min). The samples were then held in constant current mode at 17 mA for 20 min, then adjusted to 37 mA, and continued until the electrophoresis was complete. The samples were stained with Coomassie bright blue G-250 overnight and decolorized with a decolorizing solution several times until the bands were evident. The gel sections were observed with a gel imager (iBright CL1000, Thermo Fisher Scientific, Waltham, Massachusetts, USA), and the protein subunit content of the sample was analyzed.

### 2.4. Preparation of thermotropic nanoparticles

Based on the approach of Li et al. (2022) with some slight modifications, first, four accurately weighed SPIs were dissolved in room temperature deionized water to make a 2% solution of SPI, stirred for 120 min, and then stored in a refrigerator at 4 °C overnight for hydration. In four kinds of solutions, 0.02% $NaN_3$ was added to inhibit the growth of microorganisms in the solution. The pH was adjusted to 7.0 for the four protein solutions, and the solutions were centrifuged again at 14,000×*g* for 30 min (Allegra X-22, Beijing Dongxun Tiandi Medical Instrument Co., LTD, Beijing, China) to remove insoluble material. Finally, these four SPI solutions were heated and stirred in a water bath at 95 °C for 30 min, and immediately after heating, the solutions were cooled to room temperature and freeze-dried. The solutions were named Wild-NPs, α-lack-NPs, α′-lack-NPs and (α + α′)-lack-NPs for later data processing.

### 2.5. Fourier transform infrared spectroscopy

FTIR spectra of samples were recorded using a Bio-Rad FTS-60A FTIR spectrum meter according to the method of Huang, Bekiaris, Fitamo, Scheutz, and Bruun (2021) with slight modifications. Four kinds of protein nanoparticles (1 mg each) and 100 mg potassium bromide (KBr) were fully ground and placed in a thin sheet. The sample was scanned 48 times at a temperature of 25 °C, a scanning range of 4000–400 $cm^{-1}$, a wavenumber accuracy setting of 0.01 $cm^{-1}$, and a resolution of 4 $cm^{-1}$.

### 2.6. Particle size and ζ-potential

Based on this method of Igartúa, Platania, Balcone, Palazolo, and Cabezas (2022), at room temperature, Wild-NPs, α-lack-NPs, α′-lack-NPs, and (α + α′)-lack-NPs were hydrated with deionized water, stirred continuously for 2 h to ensure adequate protein solubilization, and then hydrated at 4 °C. The sample solutions were diluted 100-fold, and the mean particle size and ζ-potential were determined by dynamic optical scattering and a particle size analyzer (173plus, Brookhaven Instruments Corporation, Austin, Texas USA).

### 2.7. Surface hydrophobicity ($H_0$)

The method of Zhang, Chen, Qi, Sui, and Jiang (2018) with minor modifications was used to determine surface hydrophobicity using a 1-anilinonaphthalene-8-sulfonic acid (ANS) fluorescent probe. Briefly, Wild-NPs, α-lack-NPs, α′-lack-NPs, and (α + α′)-lack-NPs were then dissolved in 10 mmol/L PBS at pH 7.0 to obtain 1 mg/mL protein solutions, which were then diluted to various concentrations (0.1, 0.2, 0.3, 0.4, 0.5 mg/mL). Two milliliters of the diluted SPI solution were mixed with 25 μL of 8.0 mmol/L ANS at pH 7.0. After 0.5 h of reaction in darkness, the fluorescence intensities of the four samples were measured at 390 nm (excitation wavelength), 470 nm (emission wavelength), and 5 nm (slit

width). The recorded fluorescence intensities were plotted against protein concentrations and linearly fitted with slopes corresponding to the surface hydrophobicity of the proteins.

### 2.8. Contact angle (θ)

The contact angle was measured based on the method described by Meng et al. (2022) with a few modifications. The sample powders of Wild-NPs, α-lack-NPs, α′-lack-NPs, and (α + α′)-lack-NPs were pressed into thin sheets. Ten microliters of distilled water were applied to the sample surface using a high-precision syringe. The images of the resulting three-phase contact angle (θ) were recorded simultaneously by a high-speed camera equipped with an image analysis system.

### 2.9. Preparation of Pickering emulsion

The Pickering Emulsion was made based on Ji et al.'s (2022) method with slight modification, and the prepared solution of raw thermal nanoparticles as an aqueous solution and the addition of 20% (v/v) soybean oil as the oil phase and then a high-speed shear emulsifier was added (Ultra-Turrax T10, Germany IKA Instrument Equipment Co., LTD, Staufen, Germany). The colostrum was then homogenized 3 times at 400 bar using a high-pressure homogenizer (ULTRA-TURRAX UTL 2000, Germany IKA Instrument Equipment Co., LTD, Staufen, Germany) to prepare Pickering emulsions with different subunit deletion types of soy protein. The Pickering emulsions were kept sealed and stored at 4 °C. These Pickering emulsions were labeled Wild-NPPEs, α-lack-NPPEs, α′-lack-NPPEs and (α + α′)-lack-NPPEs for later data processing.

### 2.10. Rheological properties

According to Zhang et al. (2022), the apparent viscosities were measured at 25 °C using a Bohlin CVO rotational rheometer (Malvern Instruments, Shanghai, China) with a parallel plate of d = 40 mm and a gap of 1.0 mm. The apparent viscosities were measured in the range of shear rates from 0.1 to 100 $s^{-1}$ by taking an appropriate amount of sample on the parallel plate. The energy storage modulus G' and loss modulus G'' were measured at 1% constant strain and 0.1 ~ 100 Hz dynamic frequency scan range.

### 2.11. Emulsification activity index (EAI) and emulsion stability index (ESI) of Pickering emulsions

The determination was carried out based on the approach of Wang et al. (2022) with minor modifications by preparing a 0.1% (w/v) sodium dodecyl sulfate (SDS) solution, diluting the freshly prepared emulsion to 0.1 mg/ml and shaking well to mix. The absorbance $A_0$ was measured at a wavelength of 500 nm using 0.1% (w/v) SDS solution as a blank, and the absorbance $A_{10}$ was measured after standing for 10 min. The EAI and ESI were calculated as follows.

$$\mathrm{EAI}\ (m^2/g) = \frac{2 \times T \times A_0 \times N}{C \times \theta \times L \times 10000} \quad (1)$$

$$\mathrm{ESI}\ (\mathrm{min}) = \frac{A_0}{A_0 - A_{10}} \times 10 \quad (2)$$

where $A_0$ - absorbance at 0 min

T - 2.303
N - dilution times
C - concentration of protein (g/mL)
θ - the proportion of the oil phase
L - cuvette optical path length
$A_{10}$ - absorbance at 10 min.

### 2.12. Confocal laser scanning microscopy (CLSM)

The method of Shen et al. (2022) was slightly modified to view the morphology of the emulsion using laser confocal microscopy (SP8, Germany IKA Instrument Equipment Co., LTD, Staufen, Germany. A staining solution containing 1 mg Nile Red and 1 mg Nile Blue was prepared in 1 mL of ethanol and added to the emulsion (1:4) for 1 h. The dyed Pickering emulsion was then dropped into a slot on a groove on the slide, covered, and observed at excitation wavelengths of 488 nm and 633 nm.

### 2.13. Stability of Pickering emulsions

Four kinds of freshly prepared Pickering emulsions were stored in centrifugal tubes at 4 °C and 25 °C, and the Creaming Index (CI) was calculated on Days 1, 3, 5, 7, 15, and 30. According to the method of Niu et al. (2022), the emulsion was added to a 10 mL centrifuge tube, and the total height $H_l$ (cm) and $H_t$ clear liquid height (cm) of the emulsion were measured with a ruler to analyze its stability.

$$\mathrm{CI} = \frac{H_l}{H_t} \times 100\% \quad (3)$$

where $H_l$ is the height of the lower liquid layer.

$H_t$ is the total height of the emulsion.

### 2.14. Statistical analysis

The experiments described above were performed in three replications, and statistical calculations (ANOVA) were applied using the SPSS 22.0 software program (IBM Corporation, Armonk, New York, USA). Statistical values were usually set at $p < 0.05$.

The specific results of 3 unbiased replicates are presented as the mean ± standard variance. Data were analyzed and drawn by using Origin 8.5 software.

## 3. Results and discussion

### 3.1. SDS–PAGE

The SDS–PAGE electrophoresis profiles of soybean and SPI with four different subunit deficiencies are shown in Fig. 1. The main components of soy protein are β-conglycinin (7S globulin) and soy globulin (11S globulin), where 7S globulin is a trimer containing three subunits, α, α′, and β (molecular weight in the range of 48–100 kDa). 11S globulin is composed of acidic subunit A (molecular weight at approximately 35 kDa) bridged by disulfide bonds and essential peptides B (at a molecular weight of approximately 17 kDa) consisting of a hexamer (Hu et al., 2023). The characteristic bands of four of these soybeans and SPI were consistent with the findings of previous studies (Shen et al., 2022; Wang et al., 2021).

### 3.2. Particle size and ζ-potential

As shown in Fig. 2A, the α′-lack-NPs formed under heating at 95 °C for 30 min had a maximum particle size of 385.33 nm. This result was once consistent with the findings of Guo et al. (2021). This may be because the heating treatment allowed the protein to transition from the small molecule shape to the polymer structure, exposing a massive wide variety of its hydrophobic groups. According to Chevalier and Bolzinger (2013):

$$\Delta E = \pi r^2 \gamma (1 - |\cos\theta|)^2 \quad (4)$$

The smaller the particle size of the nanoparticles is, the larger the contact area with oil and water, so the more significant the requirement for

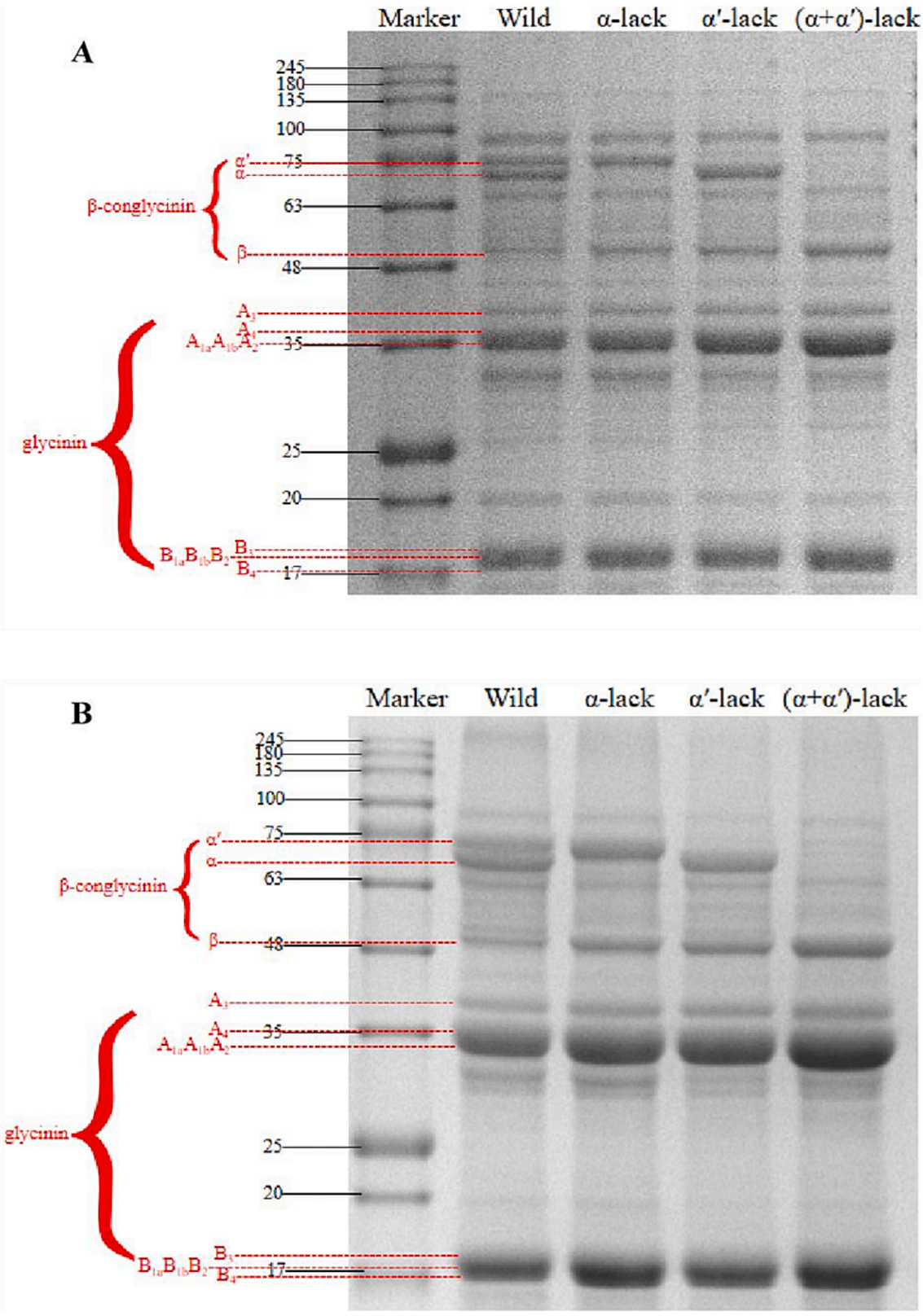


**Fig. 1.** SDS-PAGE electrophoresis patterns of four different subunit deletion types. (A: soybean; B: soybean protein isolate).

energy for the successful desorption of particles at the interface between oil and water (Wang et al., 2022). In this study, α′-lack-NPs has a larger average size than the others, which means it can have higher desorption energy from the interface between oil and water, and the more significant energy of desorption may favor the stabilization of Pickering emulsions (Wu et al., 2015). Additionally, ζ-potential is an important index of the stability of the dispersion system. The larger the absolute value of ζ-potential, the more stable the dispersion system is; the smaller the absolute value, the greater the system is dispersed, and the more it tends to coalesce or condense (Wong, Day, & Augustin, 2011). The

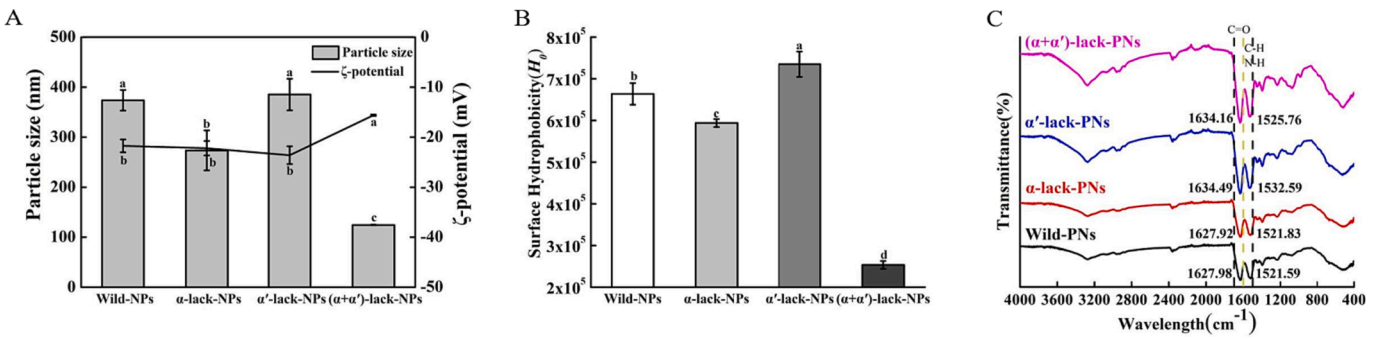


**Fig. 2.** The characteristics of α and α′ subunit deletion soybean protein nanoparticles. A: Effects of deletion of α and α′ subunits on the particle size and ζ-potential; B: Analysis of surface hydrophobicity; C: Fourier transforms infrared spectroscopy analysis. Different letters represent significant differences ($p < 0.05$).

ζ-potential of all samples was negative, which may be because soy protein nanoparticles are negatively charged at pH values above that of the isoelectric point. Heat treatment operations increase the negative charge of the protein surface, which usually prevents the agglomeration of particles and improves their internal stability (Guo et al., 2021). However, the potential of (α + α′)-lack-NPs was relatively small, consistent with the results of the study by Ju et al. (2023). This may additionally be due to the surface of the protein having a less homogenous charge, which leads to the weakening of the electrostatic repulsion among protein molecules. The ζ-potential of Wild-NPs, α-lack-NPs, and α′-lack-NPs was relatively large, indicating that they have the potential to stabilize Pickering emulsions.

### 3.3. Surface hydrophobicity

The surface hydrophobicity of soy protein nanoparticles is a critical parameter affecting their surface-related functions. Surface hydrophobicity is closely associated with useful properties, such as emulsification and foaming properties (Alavi et al., 2019). As seen in Fig. 2B, the α′-lack-NPs had the highest surface hydrophobicity, possibly due to the more extended protein molecules. The surface hydrophobicity of soy protein nanoparticles with different subunit deletion types was different, which might be related to the different surface hydrophobic groups and spatial conformations of soy protein nanoparticles. Consistent with the study by Ma et al. (2022), the surface hydrophobic groups of α′-lack-NPs expose greater hydrophobic amino acids, increasing $H_0$. The greater the $H_0$ was, the more favorable the hydrophobic interactions of the protein substrates. More large molecular aggregates form in the solution, and the volumes of the soluble aggregates become larger (Fig. 2A). At the same time, more hydrophobic groups are exposed to the molecular surface, promoting the cross-linking of hydrophobic interactions between molecules and improving the structural properties (Kang et al., 2016). Therefore, the hydrophobic group exposed by α′-lack-NPs can promote the formation of a more stable structure.

### 3.4. FTIR spectroscopy

Fourier infrared (IR) spectroscopy is an effective means to study protein structures and can detect functional groups of proteins and vibrations of highly polar bonds in soy protein nanoparticles. Four soy protein nanoparticles were analyzed by FTIR spectroscopy. The results are shown in Fig. 2C. The four soy protein nanoparticles had C═O stretching (amide I), N—H bending of primary amine groups (amide I), C—N stretching, and N—H bending (amide III) bands at 1630 cm$^{-1}$ (Kang et al., 2023). Moreover, the absorption at approximately 1630 cm$^{-1}$ indicates the C═O stretching vibration, and the absorption at 1600 cm$^{-1}$ suggests the C—H stretching vibration. The peak of α′-lack-NPs in the amide I region undergoes a redshift from 1627.98 cm$^{-1}$ to 1627.92 cm$^{-1}$ relative to wild-type NPs, which may disrupt hydrophobic interactions and hydrogen bonding between protein aggregates (Zhao et al., 2021). This is probably because intermolecular hydrogen bonds were formed between free amino acid residues in the process of thermal denaturation with the expansion of its spherical folding structure. When hydrogen bonding was strong, the density of the C═O electron cloud decreased, causing absorption peaks to shift in the direction of lower wavenumbers. In contrast, α′-lack-NPs had a more stable 3D structure, indicating that the deletion of the α′ subunit affected the stability of soy protein nanoparticles (Fu et al., 2023).

### 3.5. Contact angle

To a certain extent, the contact angle shows the interface wettability and lipophilicity of the material (Destribats, Rouvet, Gehin-Delval, Schmitt, & Binks, 2014). When θ < 90°, the solid particles exhibited better hydrophilicity; when θ > 90°, the solid particles exhibited greater lipophilicity; when θ was close to 90°, the solid particles were amphiphilic, and the prepared nanoparticles had good stability (Rai Widarta, Rukmini, Santoso, Supriyadi, & Raharjo, 2022). The contact angles of four different subunit-deficient soy protein nanoparticles are shown in Fig. 3. The θ values of all samples were less than 90°, and the contact angles of Wild-NPs, α-lack-NPs, α′-lack-NPs and (α + α′)-lack-NPs were 76.49°, 76.25°, 80.69°, and 53.50°, respectively. Among them, α′-lack-NPs were the closest to 90°, which indicates that its heating rearranged the structure and exposed more of the hydrophobic amino acids on the surface. Based on the desorption energy equation (Eq. (4)), the higher the θ value of α′-lack-NPs is, the better their ability to stabilize Pickering emulsions. The reason for this is that it is relatively hydrophobic, which is consistent with the theory of Cui et al. (2023). In addition, heating

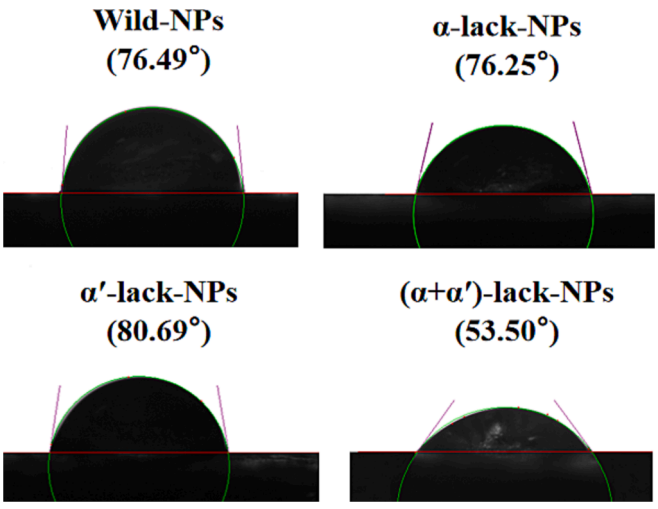


**Fig. 3.** Analysis of contact angle of α and α′ subunit deletion soy protein nanoparticles.

exposes the hydrophobic amino acids in the protein's interior, which is also in agreement with the surface hydrophobicity data (Fig. 2B). This leads to an improved affinity of the particles for the oil and thus an increase in θ (Zhou et al., 2022). Therefore, α′-lack-NPs can enhance the wettability and stability of emulsions at the interface.

### 3.6. Particle size and ζ-potential of emulsions

The smaller the particle size of the emulsion, the slower and more uniformly distributed the emulsion will be, and the emulsion will be more stable (Su et al., 2023). As shown in Fig. 4A, the particle size of α′-lack-NPPEs was the smallest, which may be attributed to the large particle size of α′-lack-NPs (Fig. 2A), and can be dispersed in the continuous phase and form a gel network due to the tight arrangement on the oil–water interface, which prevents the condensation of droplets. Thus, the particle size of the emulsion was reduced, and the stability of the emulsion was increased (Hunter, Pugh, Franks, & Jameson, 2008; Tang, 2017). Another reason could be the formation of protein thermal aggregation nanoparticles due to heat treatment, which dramatically improved the emulsifying efficiency of soybean protein, and emulsification efficiency largely due to the increase in the surface hydrophobicity, among them, α′-lack-NPs large surface hydrophobicity, increasing the stability of the emulsion. The results indicated that the α′-lacking-NPs could be better aligned at the oil–water interface, and their emulsions had smaller droplet sizes and better storage properties.

ζ-Potential is one of the most important indicators of the stability of a colloidal dispersal system and can also measure the strength of the interaction between the particles (Jeong, Oh, & Kim, 2001). The smaller the particles of an emulsion are, the higher the absolute value of the ζ-potential, and the more stable the mixed system, which allows the particles to resist aggregation when dissolved or dispersed (Mikulcová, Bordes, Minařík, & Kašpárková, 2018). When the Pickering emulsion had a high ζ-potential value, it indicated relatively good stability of the emulsion.

### 3.7. Rheological properties

One of the essential indicators of emulsion properties is the rheological properties, which are closely related to their internal system and the interaction between droplets (Zhang, Liang, & Li, 2022). As shown in Fig. 4C, the apparent viscosity of the four Pickering emulsions was inversely related to the shear rate. All of the emulsions exhibited the properties of non-Newtonian fluids (pseudoplastic fluids) (Hebishy, Buffa, Juan, Blasco-Moreno, & Trujillo, 2017), probably because the shear stress caused the protein nanoparticles and oil droplets to form aggregates that were deformed or even destroyed by the bridging interaction between them as the shear rate gradually increased (Ren et al., 2021). The highest apparent viscosity of α′-lack-NPPEs may be attributed to the vital role of the surface hydrophobicity of protein nanoparticles in the formation of gel-like network structures in the emulsions (Liu & Tang, 2016). For stable emulsions, intermolecular interactions and the formation of weak transient networks may lead to shear thinning behavior due to interactions between adjacent aggregated molecules (Dapueto, Troncoso, Mella, & Zúñiga, 2019). The results showed that α′-lack-NPPEs were conducive to maintaining better stability of the emulsion.

To better appreciate the connection between the microstructure and macroscopic properties of emulsions, dynamic viscoelasticity tests were conducted. As shown in Fig. 4C, the G′ (energy storage modulus) of all four emulsions was larger than G″ (loss modulus) and in the range of 0.1–100 Hz, indicating that the emulsions exhibited elastic behavior and had gel-like properties at this time (Ren, Chen, Zhang, Lin, & Li, 2020). Among them, the α′ subunit-deficient nanoparticle Pickering emulsion had the largest G′, which may be the result of thermal induction to increase the surface hydrophobicity of proteins (Ai, Zhang, Fan, Cao, & Jiang, 2021) (consistent with Fig. 2B). At the same time, the smaller the particles in the emulsion (Fig. 4A), the more the protein nanoparticles were allowed to adsorb at the oil–water interface and form stable network structures, which was consistent with the results from Guo, Cui, Huang, and Meng (2022). The results showed that a higher G′ (energy storage modulus) of the α′ subunit-deletion nanoparticle Pickering

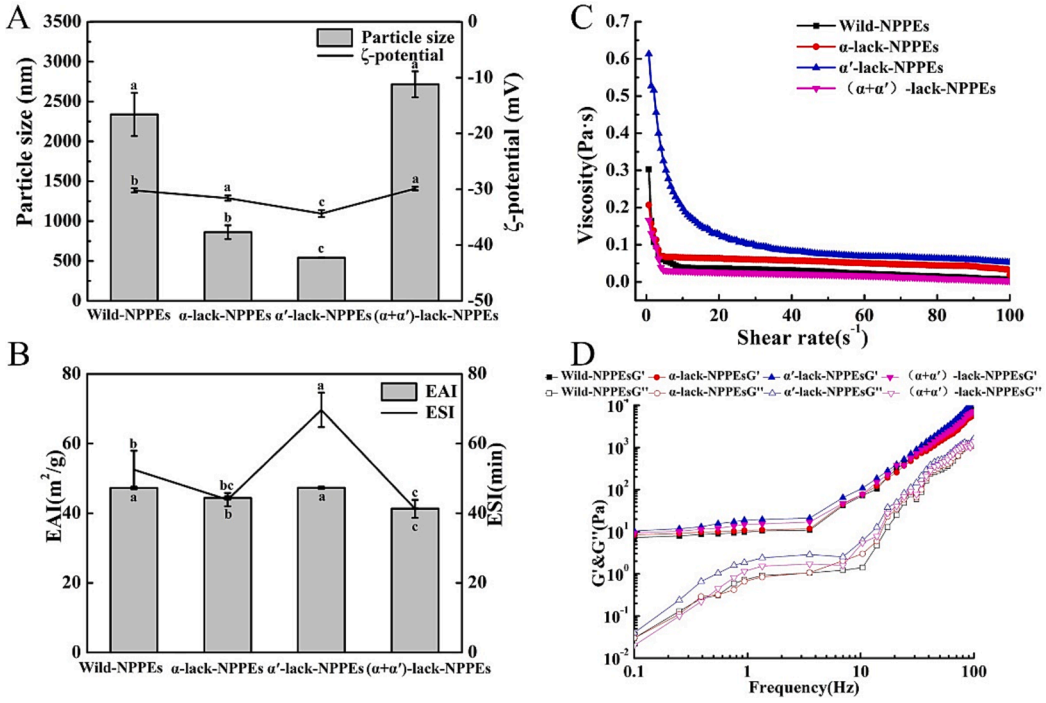


**Fig. 4.** The characteristics of α and α′ subunit deletion soy protein Pickering emulsion. A: Analysis of particle size and ζ-potential; B: Analysis of EAI, ESI; C: Change of the apparent viscosity of Pickering emulsion at shear rates of 0.1–100 $s^{-1}$. D: Pickering emulsion at angular velocities of 1–100 Hz (* G and G' represent storage modulus and loss storage, respectively). Different letters represent significant differences ($p < 0.05$).

emulsion was beneficial for the emulsion to maintain better stability.

### 3.8. Emulsifying activity and emulsification stability

The EAI is the ability of nanoparticles to be adsorbed on the oil–water interface for Pickering emulsions as well as to control the dissemination and aggregation of oil droplets. The ESI was expressed as the stability of the droplets in the emulsion (Zhang et al., 2022). As indicated in Fig. 4B, the four kinds of emulsions showed good emulsifying activity and emulsion stability. Among them, the emulsifying activity of α′-lack-NPPEs was relatively high. This may be related to their diffusion into newly formed interfaces, their expansion and repositioning in a manner that reduces interfacial tension, and their formation by polymerization of viscous and viscoelastic film aggregation, together with disulfide bonding and hydrophobic interactions (Felix, Yang, Guerrero, & Sagis, 2019). The proteins that adsorb at the oil–water interface affect the stability of emulsions, possibly through the reduction of the interfacial tension from water to oil, which is associated with the formation of viscoelastic films at the oil–water interface (Fig. 4C), as they facilitate interfacial tension reduction (Gomes, Costa, & Cunha, 2018; Zhang, Xu, Zhao, & Zhou, 2022). Additionally, combined with particle size (Fig. 2A), it can be seen that the larger the particle size of α′-lack-NPs is, the more effective the diffusion into the oil–water interface of the emulsion during the emulsification process; thus this results in the formation of smaller liquid droplets in the emulsion, reducing the particle size in the emulsion. The adsorption of α′-lack-NPs was irretrievable and therefore may be more useful in the prevention of emulsion agglomeration (Linke & Drusch, 2018).

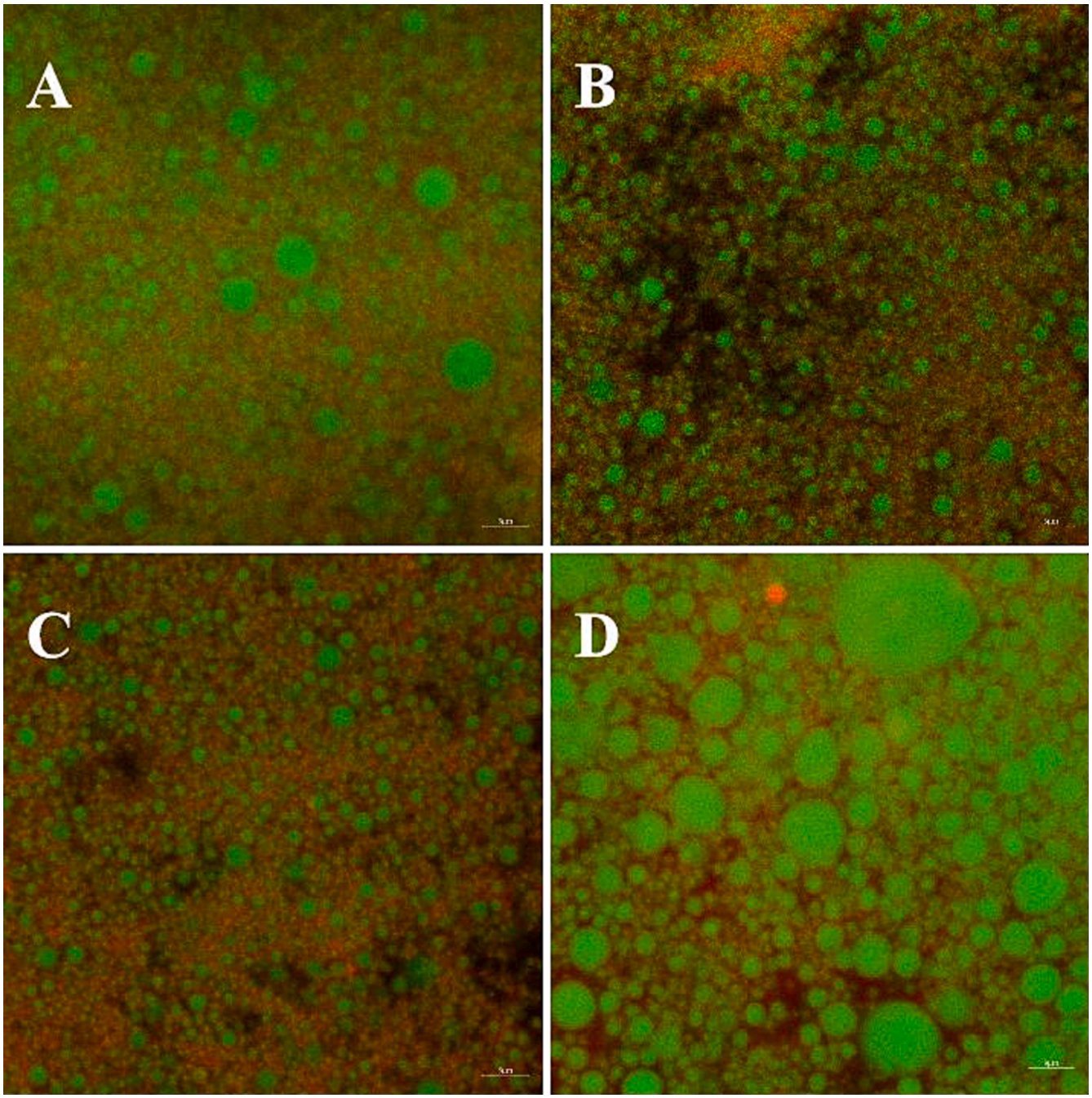


**Fig. 5.** (A) Wild nanoparticle Pickering emulsion; (B) α subunit-deletion nanoparticle. Pickering emulsion; (C) α′ subunit-deletion nanoparticle Pickering emulsion; (D) α and α′ double-subunit-deficient emulsifying.

### 3.9. CLSM images

The microstructure of Pickering emulsions prepared from different subunit-deficient soy protein nanoparticles was characterized using laser confocal microscopy (Zhang et al., 2022). As illustrated in Fig. 5, the green spherical objects in the four emulsions represented oil droplets, the red particles represented soy protein nanoparticles, and the soy protein nanoparticles surrounded the oil droplets. This adsorption promoted emulsion stability and further confirmed oil-in-water emulsion formation, in agreement with the theory from Ji et al. (2022). In this case, the droplets in the α′-lack-NPPEs were closely packed and difficult to remove. In certain situations, two adjacent droplets share the same interface layer, which forms a gel-like network structure (Zhao, Gu, Hong, Liu, & Li, 2021). This may be due to the larger particle size of nanoparticles with α′ substituent deletion, which makes the emulsion process formed by the particles and oil droplets stable by creating a dense network, providing spatial site resistance for agglomeration and Ostwald maturation and improving the stability of the emulsion (Zhu et al., 2020). The results showed that the α′ subunit-deletion nanoparticle Pickering emulsions were relatively stable.

### 3.10. Emulsion storage stability

One of the most important indicators for determining the stability of emulsions is storage stability. During storage, emulsions emerged as the obvious water–oil phase separation, mainly due to gravity, resulting in emulsions on the top of the system and precipitated water layers on the bottom (Zhu, Zheng, Song, Ren, & Gong, 2020). When the value of CI was quantified, the higher the value was, the higher the phase separation and the relatively poor storage stability of the emulsion (Hong, Kim, & Lee, 2018). As shown in Fig. 6, the phenomena of Wild-NPPEs, α-lack-NPPEs, α′-lack-NPPEs, and (α + α′)-lack-NPPEs occurred on the 5th, 7th, 15th, and 3rd days, respectively. Furthermore, the CI value increased with storage time. Among them, α′-lack-NPPEs had a relatively small creaming index, so its emulsion was more stable at Day 30. According to Stokes' law, an enhancement in emulsion viscosity (Fig. 4C) or a decrease in droplet size (Fig. 4A) can prevent gravitational separation (Wang, Zhang, Chen, He, & Ju, 2020). In addition, because the protein nanoparticles adsorbed at the oil–water interface, they may have a larger particle size and more considerable desorption energy, which is not accessible to desorption, which will make the interfacial film formed between oil and water thicker, and the steric hindrance formed will be enhanced, thus increasing the ability to block the polymerization between oil droplets, consistent with the results of Wu et al. (2022). Indeed, as shown in Fig. 5, the protein particles in Pickering emulsions are tightly bound to the oil droplets, and the gel-like network structure is more stable, providing an effective impediment to the free movement of droplets and promoting long-term stability (Zhao, Fan, Liu, & Li, 2023).

## 4. Conclusions

This study investigated the application of different subunit-deficient soybean isolated proteins (Wild-NPs, α-lack-NPs, α′-lack-NPs and (α + α′)-lack-NPs) in food Pickering emulsions. In this study, thermal induction of α′ subunit-deletion proteins was prepared to produce α′-lack-NPs with the largest size (385.33 nm) with good surface hydrophobicity and particle wettability. In addition, the heating treatment promoted the formation of protein interconnections, which resulted in good stability of the prepared emulsions (Wild-NPPEs, α-lack-NPPEs, α′-lack-NPPEs and (α + α′)-lack-NPPEs) in terms of particle size, potential, EAI, ESI, and rheological behavior, and the clustering of oil droplets and protein nanoparticles in the emulsions can also be observed by CLSM, indicating good stability. The α′ subunit-deletion soybean isolate stabilizes Pickering emulsions with good stability and potential for innovative new applications in food formulations. In the present study the production of food-grade α′ subunit-deletion soybean isolates can be used as an effective emulsion stabilizer compared with the wild type and provides a prospective strategy. In this study, the effects on the stability of Pickering emulsion were discussed in terms of variety and raw protein composition, but the effects of processing methods on the product were not considered in this study. Therefore, one of the next targets is the influence of raw material properties and processing methods on emulsion stability.

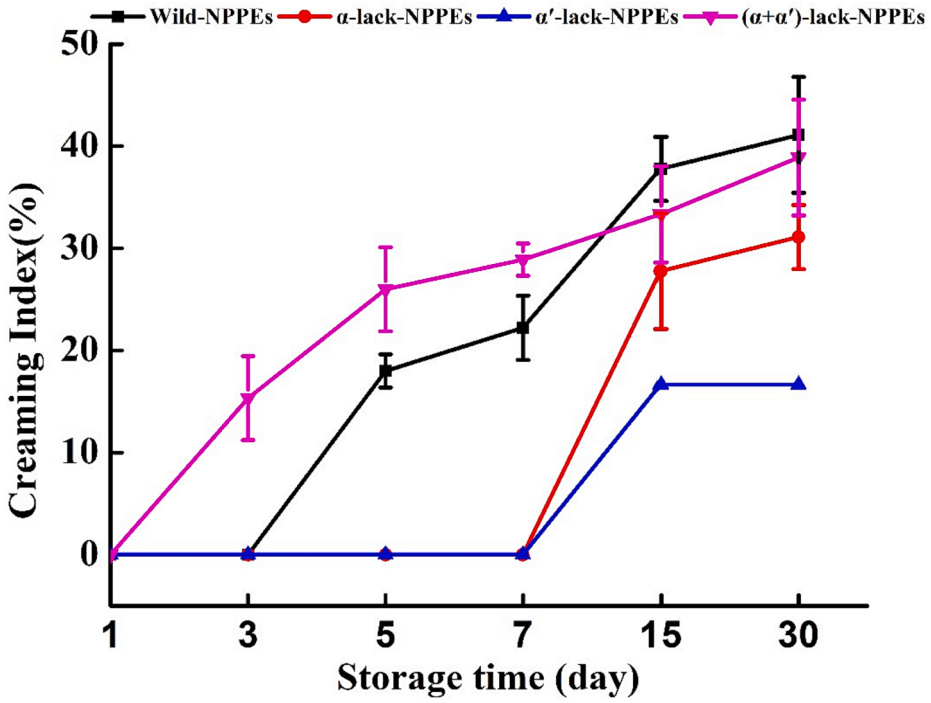


**Fig. 6.** Analysis of storage stability of Pickering emulsion with α and α′ subunit deletion of soy protein.

## CRediT authorship contribution statement

**Chunmei Gu:** Methodology, Writing – original draft. **Pengchao Dong:** Conceptualization, Methodology, Software, Formal analysis. **Feihong Jiang:** Data curation, Software. **Hongling Fu:** Writing – review & editing, Visualization. **Bo Lyu:** Validation. **Haoming Li:** Software. **Youbao Li:** Software. **Hansong Yu:** Funding acquisition, Supervision. **Weichang Dai:** Funding acquisition, Data curation, Supervision.

## Declaration of Competing Interest

The authors declare that they have no known competing financial interests or personal relationships that could have appeared to influence the work reported in this paper.

## Data availability

Data will be made available on request.

## Acknowledgments

This work was supported by the China Agriculture Research System of MOF and MARA (Project No. CARS-04), the Science and Technology Department Plan Project of Jilin Province (20220203985F). The different soybean varieties were provided by the team of Prof. Shanshan Liu & and Dr. Bo Song from the Key Laboratory of Soybean Biology in the Chinese Ministry of Education, College of Agriculture, Northeast Agricultural University (Harbin, China). We would like to thank them for their continuous support for this study.

## References

Ai, M., Zhang, Z., Fan, H., Cao, Y., & Jiang, A. (2021). High-intensity ultrasound together with heat treatment improves the oil-in-water emulsion stability of egg white protein peptides. *Food Hydrocolloids, 111*, Article 106256. https://doi.org/10.1016/j.foodhyd.2020.106256

Aimable, A., Lecomte-Nana, G., & Pagnoux, C. (2022). Chapter 9 - Role of surfactants and polymers for clay minerals as stabilizer of Pickering emulsion. In F. Wypych & R. A. de Freitas (Eds.), *Developments in clay science* (Vol. 10, pp. 277-314): Elsevier. https://doi.org/10.1016/B978-0-323-91858-9.00007-0.

Alavi, F., Emam-Djomeh, Z., Momen, S., Mohammadian, M., Salami, M., & Moosavi-Movahedi, A. A. (2019). Effect of free radical-induced aggregation on physicochemical and interface-related functionality of egg white protein. *Food Hydrocolloids, 87*, 734–746. https://doi.org/10.1016/j.foodhyd.2018.08.048

Amar Feldbaum, R., Yaakov, N., Ananth Mani, K., Yossef, E., Metbeev, S., Zelinger, E., … Mechrez, G. (2021). Single cell encapsulation in a Pickering emulsion stabilized by TiO2 nanoparticles provides protection against UV radiation for a biopesticide. *Colloids and Surfaces B: Biointerfaces, 206*, Article 111958. https://doi.org/10.1016/j.colsurfb.2021.111958

Cen, K., Yu, X., Gao, C., Feng, X., & Tang, X. (2021). Effects of different vegetable oils and ultrasonicated quinoa protein nanoparticles on the rheological properties of Pickering emulsion and freeze-thaw stability of emulsion gels. *Journal of Cereal Science, 102*, Article 103350. https://doi.org/10.1016/j.jcs.2021.103350

Chevalier, Y., & Bolzinger, M.-A. (2013). Emulsions stabilized with solid nanoparticles: Pickering emulsions. *Colloids and Surfaces A: Physicochemical and Engineering Aspects, 439*, 23–34. https://doi.org/10.1016/j.colsurfa.2013.02.054

Cui, S., McClements, D. J., Shi, J., Xu, X., Ning, F., Liu, C., … Dai, L. (2023). Fabrication and characterization of low-fat Pickering emulsion gels stabilized by zein/phytic acid complex nanoparticles. *Food Chemistry, 402*, Article 134179. https://doi.org/10.1016/j.foodchem.2022.134179

Dapueto, N., Troncoso, E., Mella, C., & Zúñiga, R. N. (2019). The effect of denaturation degree of protein on the microstructure, rheology and physical stability of oil-in-water (O/W) emulsions stabilized by whey protein isolate. *Journal of Food Engineering, 263*, 253–261. https://doi.org/10.1016/j.jfoodeng.2019.07.005

Destribats, M., Rouvet, M., Gehin-Delval, C., Schmitt, C., & Binks, B. P. (2014). Emulsions stabilised by whey protein microgel particles: Towards food-grade Pickering emulsions. *Soft matter, 10*(36), 6941–6954. https://doi.org/10.1039/C4SM00179F

Felix, M., Yang, J., Guerrero, A., & Sagis, L. M. C. (2019). Effect of cinnamaldehyde on interfacial rheological properties of proteins adsorbed at O/W interfaces. *Food Hydrocolloids, 97*, Article 105235. https://doi.org/10.1016/j.foodhyd.2019.105235

Fu, H., Li, J., Yang, X., Swallah, M. S., Gong, H., Ji, L., … Yu, H. (2023). The heated-induced gelation of soy protein isolate at subunit level: Exploring the impacts of α and α′ subunits on SPI gelation based on natural hybrid breeding varieties. *Food Hydrocolloids, 134*, Article 108008. https://doi.org/10.1016/j.foodhyd.2022.108008

Gomes, A., Costa, A. L. R., & Cunha, R. L. (2018). Impact of oil type and WPI/Tween 80 ratio at the oil-water interface: Adsorption, interfacial rheology and emulsion features. *Colloids and Surfaces B: Biointerfaces, 164*, 272–280. https://doi.org/10.1016/j.colsurfb.2018.01.032

Guo, J., Cui, L., Huang, Y., & Meng, Z. (2022). Spirulina platensis protein isolate nanoparticle stabilized O/W Pickering emulsions: Interfacial adsorption and bulk aggregation. *Food Research International, 161*, Article 111815. https://doi.org/10.1016/j.foodres.2022.111815

Guo, Z., Huang, Z., Guo, Y., Li, B., Yu, W., Zhou, L., … Wang, Z. (2021). Effects of high-pressure homogenization on structural and emulsifying properties of thermally soluble aggregated kidney bean (Phaseolus vulgaris L.) proteins. *Food Hydrocolloids, 119*, Article 106835. https://doi.org/10.1016/j.foodhyd.2021.106835

Hebishy, E., Buffa, M., Juan, B., Blasco-Moreno, A., & Trujillo, A.-J. (2017). Ultra high-pressure homogenized emulsions stabilized by sodium caseinate: Effects of protein concentration and pressure on emulsions structure and stability. *LWT - Food Science and Technology, 76*, 57–66. https://doi.org/10.1016/j.lwt.2016.10.045

Hong, I. K., Kim, S. I., & Lee, S. B. (2018). Effects of HLB value on oil-in-water emulsions: Droplet size, rheological behavior, zeta-potential, and creaming index. *Journal of Industrial and Engineering Chemistry, 67*, 123–131. https://doi.org/10.1016/j.jiec.2018.06.022

Hu, M., Yue, Q., Liu, G., Jia, Y., Li, Y., & Qi, B. (2023). Complexation of β-conglycinin or glycinin with sodium alginate blocks: Complexation mechanism and structural and functional properties. *Food Chemistry, 403*, Article 134425. https://doi.org/10.1016/j.foodchem.2022.134425

Huang, J., Bekiaris, G., Fitamo, T., Scheutz, C., & Bruun, S. (2021). Prediction of biochemical methane potential of urban organic waste using Fourier transform mid-infrared photoacoustic spectroscopy and multivariate analysis. *Science of The Total Environment, 790*, Article 147959. https://doi.org/10.1016/j.scitotenv.2021.147959

Huang, Q., Lee, Y. Y., Wang, Y., & Qiu, C. (2023). Structural characterization, interfacial and emulsifying properties of soy protein hydrolysate-tannic acid complexes. *Food Hydrocolloids, 137*. https://doi.org/10.1016/j.foodhyd.2022.108415

Hunter, T. N., Pugh, R. J., Franks, G. V., & Jameson, G. J. (2008). The role of particles in stabilising foams and emulsions. *Advances in Colloid and Interface Science, 137*(2), 57–81. https://doi.org/10.1016/j.cis.2007.07.007

Igartúa, D. E., Platania, F. A., Balcone, A., Palazolo, G. G., & Cabezas, D. M. (2022). Impact of heat treatment in whey proteins-soluble soybean polysaccharides electrostatic complexes in different pH and biopolymer mass ratio conditions. *Applied Food Research, 2*(2), Article 100184. https://doi.org/10.1016/j.afres.2022.100184

Jeong, M.-W., Oh, S.-G., & Kim, Y. C. (2001). Effects of amine and amine oxide compounds on the zeta-potential of emulsion droplets stabilized by phosphatidylcholine. *Colloids and Surfaces A: Physicochemical and Engineering Aspects, 181*(1), 247–253. https://doi.org/10.1016/S0927-7757(00)00796-2

Ji, Y., Han, C., Liu, E., Li, X., Meng, X., & Liu, B. (2022). Pickering emulsions stabilized by pea protein isolate-chitosan nanoparticles: Fabrication, characterization and delivery EPA for digestion in vitro and in vivo. *Food Chemistry, 378*, Article 132090. https://doi.org/10.1016/j.foodchem.2022.132090

Ju, Q., Yuan, Y., Wu, C., Hu, Y., Zhou, S., & Luan, G. (2023). Heat-induced aggregation of subunits/polypeptides of soybean protein: Structural and physicochemical properties. *Food Chemistry, 405*, Article 134774. https://doi.org/10.1016/j.foodchem.2022.134774

Kang, D.-C., Zou, Y.-H., Cheng, Y.-P., Xing, L.-J., Zhou, G.-H., & Zhang, W.-G. (2016). Effects of power ultrasound on oxidation and structure of beef proteins during curing processing. *Ultrasonics Sonochemistry, 33*, 47–53. https://doi.org/10.1016/j.ultsonch.2016.04.024

Kang, L., Liang, Q., Chen, H., Zhou, Q., Chi, Z., Rashid, A., … Ren, X. (2023). Insights into ultrasonic treatment on the properties of pullulan/oat protein/nisin composite film: Mechanical, structural and physicochemical properties. *Food Chemistry, 402*, Article 134237. https://doi.org/10.1016/j.foodchem.2022.134237

Laemmli, U. K. (1970). Cleavage of structural proteins during the assembly of the head of bacteriophage T4. *Nature, 227*(5259), 680–685. https://doi.org/10.1038/227680a0

Li, F., Li, X., Huang, K., Luo, Y., & Mei, X. (2021). Preparation and characterization of pickering emulsion stabilized by hordein-chitosan complex particles. *Journal of Food Engineering, 292*, Article 110275. https://doi.org/10.1016/j.jfoodeng.2020.110275

Li, S., Jiao, B., Meng, S., Fu, W., Faisal, S., Li, X., … Wang, Q. (2022). Edible mayonnaise-like Pickering emulsion stabilized by pea protein isolate microgels: Effect of food ingredients in commercial mayonnaise recipe. *Food Chemistry, 376*, Article 131866. https://doi.org/10.1016/j.foodchem.2021.131866

Linke, C., & Drusch, S. (2018). Pickering emulsions in foods-opportunities and limitations. *Critical Reviews in Food Science and Nutrition, 58*(12), 1971–1985.

Liu, F., & Tang, C.-H. (2016). Soy glycinin as food-grade Pickering stabilizers: Part. III. Fabrication of gel-like emulsions and their potential as sustained-release delivery systems for β-carotene. *Food Hydrocolloids, 56*, 434–444. https://doi.org/10.1016/j.foodhyd.2016.01.002

Ma, R., Zeng, M., Huang, D., Wang, J., Cheng, Z., & Wang, Q. (2021). Amphiphilicity-adaptable graphene quantum dots to stabilize pH-responsive pickering emulsions at a very low concentration. *Journal of Colloid and Interface Science, 601*, 106–113. https://doi.org/10.1016/j.jcis.2021.05.104

Ma, Y., Qing, M., Zang, J., Shan, A., Zhang, H., Chi, Y., … Gao, X. (2022). Molecular interactions in the dry heat-facilitated hydrothermal gel formation of egg white protein. *Food Research International, 162*, Article 112058. https://doi.org/10.1016/j.foodres.2022.112058

Meng, X., Liu, H., Dong, X., Wang, Q., Xia, Y., & Hu, X. (2022). A soft Pickering emulsifier made from chitosan and peptides endows stimuli-responsiveness, bioactivity and biocompatibility to emulsion. *Carbohydrate Polymers, 277*, Article 118768. https://doi.org/10.1016/j.carbpol.2021.118768

Mikulcová, V., Bordes, R., Minařík, A., & Kašpárková, V. (2018). Pickering oil-in-water emulsions stabilized by carboxylated cellulose nanocrystals – Effect of the pH. *Food Hydrocolloids, 80*, 60–67. https://doi.org/10.1016/j.foodhyd.2018.01.034

Niu, B., Chen, H., Wu, W., Fang, X., Mu, H., Han, Y., & Gao, H. (2022). Co-encapsulation of chlorogenic acid and cinnamaldehyde essential oil in Pickering emulsion stablized by chitosan nanoparticles. *Food Chemistry: X, 14*, Article 100312. https://doi.org/10.1016/j.fochx.2022.100312

Rai Widarta, I. W., Rukmini, A., Santoso, U., Supriyadi, & Raharjo, S. (2022). Optimization of oil-in-water emulsion capacity and stability of octenyl succinic anhydride-modified porang glucomannan (Amorphophallus muelleri Blume). *Heliyon, 8*(5), Article e09523. https://doi.org/10.1016/j.heliyon.2022.e09523

Ren, Z., Chen, Z., Zhang, Y., Lin, X., & Li, B. (2020). Characteristics and rheological behavior of Pickering emulsions stabilized by tea water-insoluble protein nanoparticles via high-pressure homogenization. *International Journal of Biological Macromolecules, 151*, 247–256. https://doi.org/10.1016/j.ijbiomac.2020.02.090

Ren, Z., Chen, Z., Zhang, Y., Lin, X., Li, Z., Weng, W., … Li, B. (2021). Effect of heat-treated tea water-insoluble protein nanoparticles on the characteristics of Pickering emulsions. *LWT, 149*, Article 111999. https://doi.org/10.1016/j.lwt.2021.111999

Shen, Q., Xiong, T., Zheng, W., Luo, Y., Peng, W., Dai, J., … Chen, Y. (2022). The effects of thermal treatment on emulsifying properties of soy protein isolates: Interfacial rheology and quantitative proteomic analysis. *Food Research International, 157*, Article 111326. https://doi.org/10.1016/j.foodres.2022.111326

Slavova, D., Pollak, S., & Petermann, M. (2019). Phase inversion and rheological behavior of emulsions stabilized by silica nanoparticles and nanoclay. *Journal of Petroleum Science and Engineering, 177*, 624–633. https://doi.org/10.1016/j.petrol.2019.02.071

Su, D., Mo, H., Huang, J., Li, Q., Zhong, H., & Jin, B. (2023). Soy protein/β-glucan/tannic acid complex coacervates with different micro-structures play key roles in the rheological properties, tribological properties, and the storage stability of Pickering high internal phase emulsions. *Food Chemistry, 401*, Article 134168. https://doi.org/10.1016/j.foodchem.2022.134168

Sun, F., Li, B., Guo, Y., Wang, Y., Cheng, T., Yang, Q., … Wang, Z. (2022). Effects of ultrasonic pretreatment of soybean protein isolate on the binding efficiency, structural changes, and bioavailability of a protein-luteolin nanodelivery system. *Ultrasonics Sonochemistry, 88*, Article 106075. https://doi.org/10.1016/j.ultsonch.2022.106075

Tang, C.-H. (2017). Emulsifying properties of soy proteins: A critical review with emphasis on the role of conformational flexibility. *Critical Reviews in Food Science and Nutrition, 57*(12), 2636–2679. https://doi.org/10.1080/10408398.2015.1067594

Wang, T., Wang, N., Li, N., Ji, X., Zhang, H., Yu, D., & Wang, L. (2022). Effect of high-intensity ultrasound on the physicochemical properties, microstructure, and stability of soy protein isolate-pectin emulsion. *Ultrasonics Sonochemistry, 82*, Article 105871. https://doi.org/10.1016/j.ultsonch.2021.105871

Wang, W., Zhang, J., Zhang, X., Guo, Y., Shi, J., Shen, S., … Dou, H. (2021). Asymmetrical flow field-flow fractionation combined with electrophoresis: A new approach for studying thermal aggregation behavior of soy protein isolate. *Food Hydrocolloids, 119*, Article 106857. https://doi.org/10.1016/j.foodhyd.2021.106857

Wang, Z., Babadagli, T., & Maeda, N. (2021). Generation of pickering emulsions by activating natural asphaltenes as nano materials: An experimental analysis for cost-effective heavy-oil recovery. *Journal of Molecular Liquids, 339*, Article 116759. https://doi.org/10.1016/j.molliq.2021.116759

Wang, Z., Zhang, N., Chen, C., He, R., & Ju, X. (2020). Rapeseed protein nanogels as novel pickering stabilizers for oil-in-water emulsions. *Journal of Agricultural and Food Chemistry, 68*(11), 3607–3614. https://doi.org/10.1021/acs.jafc.0c00128

Wong, B. T., Day, L., & Augustin, M. A. (2011). Deamidated wheat protein–dextran Maillard conjugates: Effect of size and location of polysaccharide conjugated on steric stabilization of emulsions at acidic pH. *Food Hydrocolloids, 25*(6), 1424–1432. https://doi.org/10.1016/j.foodhyd.2011.01.017

Wu, B., Zhang, S., Jiang, X., Hou, P., Xin, Y., Zhang, L., … Zhou, D. (2022). Impact of weakly charged insoluble karaya gum on zein nanoparticle and mechanism for stabilizing Pickering emulsions. *International Journal of Biological Macromolecules, 222*, 121–131. https://doi.org/10.1016/j.ijbiomac.2022.09.066

Wu, J., Shi, M., Li, W., Zhao, L., Wang, Z., Yan, X., … Li, Y. (2015). Pickering emulsions stabilized by whey protein nanoparticles prepared by thermal cross-linking. *Colloids and Surfaces B: Biointerfaces, 127*, 96–104. https://doi.org/10.1016/j.colsurfb.2015.01.029

Xiao, J., Wang, X. A., Perez Gonzalez, A. J., & Huang, Q. (2016). Kafirin nanoparticles-stabilized Pickering emulsions: Microstructure and rheological behavior. *Food Hydrocolloids, 54*, 30–39. https://doi.org/10.1016/j.foodhyd.2015.09.008

Zhang, L., Liang, R., & Li, L. (2022). The interaction between anionic polysaccharides and legume protein and their influence mechanism on emulsion stability. *Food Hydrocolloids, 131*, Article 107814. https://doi.org/10.1016/j.foodhyd.2022.107814

Zhang, W., Xu, X., Zhao, X., & Zhou, G. (2022). Insight into the oil polarity impact on interfacial properties of myofibrillar protein. *Food Hydrocolloids, 128*, Article 107563. https://doi.org/10.1016/j.foodhyd.2022.107563

Zhang, Y., Chen, S., Qi, B., Sui, X., & Jiang, L. (2018). Complexation of thermally-denatured soybean protein isolate with anthocyanins and its effect on the protein structure and in vitro digestibility. *Food Research International, 106*, 619–625. https://doi.org/10.1016/j.foodres.2018.01.040

Zhang, Y., Duan, F., Fang, J., Lu, J., Wang, J., Zhang, J., … Fan, H. (2022). Preparation of soybean dreg fiber solid emulsifier and its effect on the stability of Pickering emulsion. *International Journal of Food Engineering*. https://doi.org/10.1515/ijfe-2021-0367

Zhao, C., Yin, H., Yan, J., Niu, X., Qi, B., & Liu, J. (2021). Structure and acid-induced gelation properties of soy protein isolate–maltodextrin glycation conjugates with ultrasonic pretreatment. *Food Hydrocolloids, 112*, Article 106278. https://doi.org/10.1016/j.foodhyd.2020.106278

Zhao, Q., Fan, L., Liu, Y., & Li, J. (2023). Mayonnaise-like high internal phase Pickering emulsions stabilized by co-assembled phosphorylated perilla protein isolate and chitosan for extrusion 3D printing application. *Food Hydrocolloids, 135*, Article 108133. https://doi.org/10.1016/j.foodhyd.2022.108133

Zhao, Q., Gu, Q., Hong, X., Liu, Y., & Li, J. (2021). Novel protein-based nanoparticles from perilla oilseed residues as sole Pickering stabilizers for high internal phase emulsions. *LWT, 145*, Article 111340. https://doi.org/10.1016/j.lwt.2021.111340

Zhou, S., Han, L., Lu, K., Qi, B., Du, X., Liu, G., … Li, Y. (2022). Whey protein isolate–phytosterols nanoparticles: Preparation, characterization, and stabilized food-grade pickering emulsions. *Food Chemistry, 384*, Article 132486. https://doi.org/10.1016/j.foodchem.2022.132486

Zhu, W., Zheng, F., Song, X., Ren, H., & Gong, H. (2020). Influence of formulation parameters on lipid oxidative stability of Pickering emulsion stabilized by hydrophobically modified starch particles. *Carbohydrate Polymers, 246*, Article 116649. https://doi.org/10.1016/j.carbpol.2020.116649

Zhu, X.-F., Zhang, N., Lin, W.-F., & Tang, C.-H. (2017). Freeze-thaw stability of pickering emulsions stabilized by soy and whey protein particles. *Food Hydrocolloids, 69*, 173–184. https://doi.org/10.1016/j.foodhyd.2017.02.001

Zhu, Y., Huan, S., Bai, L., Ketola, A., Shi, X., Zhang, X., … Rojas, O. J. (2020). High internal phase oil-in-water pickering emulsions stabilized by chitin nanofibrils: 3D structuring and solid foam. *ACS Applied Materials & Interfaces, 12*(9), 11240–11251. https://doi.org/10.1021/acsami.9b23430